

# ON THE APPLICATION OF LARGE-EDDY SIMULATION TO PARTICLE-LADEN FLOWS

**Vincenzo Armenio**

Dipartimento di Ingegneria Civile  
Università degli Studi di Trieste  
34127 Trieste, Italy  
Email: armenio@univ.trieste.it

**Ugo Piomelli**

Dept. of Mechanical Engineering  
University of Maryland  
College Park, MD 20742, USA  
Email: ugo@eng.umd.edu

**Virgilio Fiorotto**

Dipartimento di Ingegneria Civile  
Università degli Studi di Trieste  
34127 Trieste, Italy  
Email: fiorotto@utsj90.trieste.it

## ABSTRACT

*A priori* and *a posteriori* evaluation of the effect of the unresolved, subgrid, scales on the deposition of heavy particles are carried out. The deposition statistics obtained from the direct simulation of turbulent channel flow are compared with the results of two large-eddy simulations. Although the small scales, which are not resolved in the large-eddy simulations, are found to affect significantly the settling velocity, other quantities (the deposition rate and the distribution of the settled particles) are predicted accurately.

## 1 Introduction

The analysis of the settling velocity of particles in a turbulent flow is important in many engineering applications in which sedimentation and deposition occur. In the past (Reeks 1997) it has been recognized that the average settling velocity of heavy particles in a homogeneous isotropic turbulent field is the same as the falling velocity in a still fluid (the terminal velocity  $W$ ) if the turbulent field can be seen as a random uncorrelated noise. This is the case if the particle time-constant,  $\tau_p = \rho_p d_p^2 / 18 \rho_f \nu$  (where  $\rho_p$  and  $d_p$  are respectively the particle density and diameter,  $\rho_f$  is the fluid density and  $\nu$  is the kinematic viscosity of the fluid), is much larger than any integral time-scale of the flow, or if the particle inertia tends to zero (Maxey 1987). On the other hand, recent studies (Wang and Maxey 1993, Yang and Lei 1998) have shown that, in homogeneous isotropic turbulence, an ensemble of heavy particles experiences an increase of the settling velocity up to 50% if the particle time-constant is comparable to the Kolmogorov time-scale of the flow,  $\tau_k = (\nu/\epsilon)^{1/2}$  (where  $\epsilon$  is the viscous dissipation), and if  $W$  is equal to the Kolmogorov velocity scale,  $v_k = (\nu\epsilon)^{1/4}$ . This increase of the settling velocity has been found to depend on the inertial bias responsible for the accumulation of particles in the zones of low vorticity and high

strain rate (Yeh and Lei 1991, Wang and Maxey 1993, Yang and Lei 1998).

The increase of the settling velocity and its dependence on the characteristics of the flow have been clearly shown in homogeneous isotropic turbulence, where a unique value of the Kolmogorov scales can be defined. On the other hand, in wall-bounded turbulence the dissipation scales vary dramatically along the wall-normal direction, and it is not clear how the conclusions of the investigations mentioned above can be extended. Deposition and sedimentation of particles in wall bounded turbulent flows occur in many practical applications. For example, if we consider sedimentation of sand (with diameter of the order 1mm) in a settling tank, with velocity and water depth of the order of 0.2m/s and 2m respectively, an increase of the settling velocity may occur; according to the results of Wang and Maxey (1993) in homogeneous isotropic turbulence, the increase may reach the 25% during the sedimentation process.

In the past, the direct numerical simulation (DNS) of particle-laden flows has proven to be a valuable tool for the prediction of particle statistics and for the understanding of the underlying physics at low Reynolds numbers (McLaughlin 1989, Pedinotti *et al.* 1990, Elghobashi and Truesdell 1992, Squires and Eaton, 1991). However, the range of Reynolds numbers that can be studied by DNS is limited by its computational cost, which scales like the third power of the Reynolds number. A promising tool for the analysis of particle-laden flows at moderate Reynolds numbers is the large-eddy simulation (LES). Despite the success of some LES-based investigations (Yeh and Lei 1991, Wang and Squires 1996a,b), however, it has not been completely understood how the small scales of motion, which are neglected in an LES, affect the particle dispersion.

Yang and Lei (1998) performed LES computations to investigate the effect of filtering on the particle-settling velocity in homogeneous isotropic turbulence. Their calculations used

the Smagorinsky subgrid-scale (SGS) model, and showed that the requirement for an accurate evaluation of the settling velocity of an ensemble of particles is that the smallest resolved scale corresponds to a wavenumber greater than  $2.5k_w$ ,  $k_w$  being the wavenumber where the dissipation spectrum peaks. They also showed that, although the small scales may affect the particle motion, the settling velocity is governed to a much larger extent by the large, energy-carrying, scales. Recently, Armenio *et al.* (1999) carried out *a priori* tests using DNS data for fully developed channel flow at  $Re_\tau = 175$ , and *a posteriori* LES calculations to quantify the effect of filtering and subgrid-scale (SGS) modeling on the particle statistics in wall-bounded flows. They showed that, in the absence of gravity, an accurate LES is able to reproduce the most important particle statistics, *i.e.*, the one- and two-particles dispersion, the Lagrangian velocity-autocorrelation, and the Lagrangian integral time-scales, both for tracer particles and for particles with inertia.

The aim of the present paper is to investigate the effects of filtering and SGS modeling on the particle deposition in a horizontal channel flow (the gravitational force is considered to act in a direction perpendicular to the walls). First a DNS was performed; then the particles were driven by a velocity field filtered with increasing filter-widths in order to isolate the effect of the small scales of motion. Finally, two LES computations were carried out on grids corresponding to those of the filtered fields, in order to understand the effect of interpolation and modeling errors on the particle statistics.

In the next Section, the mathematical model used for the time-integration of the Eulerian velocity field and the model for the time-advancement of the particles are presented. In section 3 the results will be analyzed and discussed, and in section 4 some concluding remarks will be made.

## 2 Mathematical model

The governing equations for the problem under investigation, a fully developed turbulent channel flow, are the incompressible Navier Stokes equations:

$$\frac{\partial u_i}{\partial x_i} = 0, \quad (1)$$

$$\frac{\partial u_i}{\partial t} + \frac{\partial u_i u_j}{\partial x_j} = \delta_{i1} \Pi - \frac{\partial p}{\partial x_i} + \frac{1}{Re_\tau} \frac{\partial^2 u_i}{\partial x_j \partial x_j}. \quad (2)$$

Here,  $x$  or  $x_1$  represents the streamwise direction,  $y$  or  $x_2$  the spanwise directions, and  $z$  or  $x_3$  is the wall normal direction. The velocity components are  $u$ ,  $v$  and  $w$ , or  $u_1$ ,  $u_2$  and  $u_3$ . In (1–2),  $p$  is the pressure and  $\Pi$  is the driving force in the streamwise direction. The governing equations (1) and (2) are made dimensionless by the friction velocity  $u_\tau$  and the channel half-width  $\delta$ . The Reynolds number is defined as  $Re_\tau = u_\tau \delta / \nu$ . No-slip boundary

conditions are applied at the solid surfaces, and periodic conditions in the streamwise and spanwise directions.

In LES the flow variables are decomposed into a resolved component and a subgrid scale (unresolved) component. The resolved component is defined by the filtering operation:

$$\bar{f}(\mathbf{x}) = \int_D f(\mathbf{x}') G(\mathbf{x}, \mathbf{x}') d\mathbf{x}', \quad (3)$$

where  $G$  is the filter function, and the integral is extended to the entire computational domain  $D$ . The sharp Fourier cutoff (denoted by FC in the figures) filter, was employed in this study both for filtering the DNS data and in the LES:

$$\hat{G}_i(k_i) = \begin{cases} 1 & \text{for } k_i < K_{ci} \\ 0 & \text{otherwise,} \end{cases} \quad (4)$$

In (4)  $K_{ci} = \pi/\Delta_i$  is the cutoff wavenumber and  $\Delta_i$  the filter width in the  $i$ th direction,  $k_i$  is the wave number, and a caret denotes the Fourier coefficient of the filter function  $G_i$ .

The governing equations were integrated in time by a pseudo-spectral collocation method (Zang and Hussaini 1986) that uses a fractional step formulation. The wall-normal diffusive term is advanced by a Crank-Nicholson scheme, whereas the convective terms and the remaining diffusive ones are treated by a low-storage 3rd-order Runge-Kutta method. The space derivatives are computed spectrally, using Fourier expansions in the homogeneous directions and Chebychev polynomials in the wall-normal direction. The dimensions of the computational domain in the periodic directions were respectively  $l_x = 4\pi\delta$  and  $l_y = 4\pi\delta/3$ , and the Reynolds number was  $Re_\tau = 175$ . A  $128 \times 128 \times 97$  grid gives results in good agreement with the reference data by Kim *et al.* (1987). The grid is uniform in the  $xy$ -planes, and stretched in the  $z$ -direction by a cosine law. The grid spacings are  $\Delta x^+ \simeq 17$ ,  $\Delta y^+ \simeq 6$ ,  $0.09 < \Delta z^+ < 6$  (a plus denotes quantities normalized using  $u_\tau$  and  $\nu$ ).

With the assumption of large density ratios ( $\rho_p/\rho_f > 100$ ) and that the particle Reynolds number  $Re_p = d_p|\mathbf{v} - \mathbf{V}_p|/\nu$  is smaller than unity, the particle-motion equations are:

$$\frac{d\mathbf{V}_p(t)}{dt} = \frac{[\mathbf{v}(\mathbf{x}, t) - \mathbf{V}_p(t)] + \mathbf{W}}{\tau_p}, \quad (5)$$

$$\frac{d\mathbf{x}_p}{dt} = \mathbf{V}_p \quad (6)$$

where  $\mathbf{V}_p$  and  $\mathbf{x}_p$  are respectively the particle vector velocity and displacement,  $\mathbf{v}$  the fluid velocity at the particle location,  $\tau_p$  the particle time-constant, and  $\mathbf{W}$  is the terminal velocity defined previously.  $\mathbf{W}$  can be expressed as  $\mathbf{W} = \tau_p \mathbf{g}$  where  $\mathbf{g} \equiv (0, 0, \pm g)$  is the gravitational acceleration.

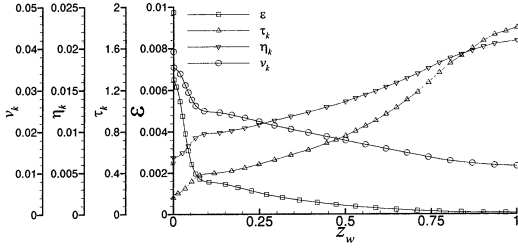


Figure 1. Variation in the wall-normal direction of the dissipation rate  $\varepsilon$ , of the Kolmogorov time-scale  $\tau_k$ , length-scale  $\eta_k$ , and velocity scale  $v_k$ .

The interpolation of the Eulerian velocity field at the particle locations was carried out by 6th-order Lagrangian polynomials in the homogeneous directions, and Chebychev polynomials in the inhomogeneous, wall-normal, one. The time-integration of (5-6) was performed using a 2nd-order Adams-Bashforth method. At the boundaries, in the  $x$ - and  $y$ -directions, a particle that moved out of the domain was re-introduced using the periodic boundary conditions, whereas a particle that reached a wall was stopped there.

The LES calculations were performed using the same numerical method as the DNS. The SGS stresses were modeled by the dynamic eddy viscosity model (Germano *et al.* 1991, Lilly 1992). The Fourier cutoff filter (4) was used in the homogeneous ( $x$  and  $y$ ) directions; no filtering was applied in the wall-normal direction. In the inhomogeneous direction the filtering operation does not commute with differentiation; thus, filtering in  $z$  would introduce additional commutation errors (Ghosal and Moin 1995), which might affect the results. Furthermore, in channel flow Murray *et al.* (1996) have shown that, for  $z^+ > 10$ , filtering in the homogeneous plane is equivalent to three-dimensional filtering.

### 3 Results and discussion

In this study 2048 particles were considered. In order to take advantage of the symmetry of the channel, the gravitational force was set positive for the first 1024 particles and negative for the remaining ones. Initially, the particles were uniformly distributed over the center plane of the channel, and their velocity was set equal to the fluid velocity at the particle location. The simulations were carried out for a non-dimensional time  $tu_\tau/\delta = 2.5$ , which was sufficient to allow the deposition of about 85% of the particles.

Figure 1 shows the wall-normal variation of the dissipation rate and of the Kolmogorov scales as a function of the distance from the wall,  $z_w = 1 - |z|/\delta$ . To allow the particles to be exposed to a wide range of the ratio  $\tau_p/\tau_k$ , the particle time-constant was set equal to the Kolmogorov time-scale evaluated

by the average dissipation rate,  $\tau_m = (\nu/\varepsilon_m)^{1/2}$ , where  $\varepsilon_m$  is the average of  $\varepsilon$  over the entire channel volume. This results in  $\tau_p = \tau_m = 0.55\delta/u_\tau$ . Similarly, in order to obtain a terminal velocity equal to the Kolmogorov velocity-scale based on  $\varepsilon_m$ ,  $v_m = (\nu\varepsilon_m)^{1/4} = 0.0209u_\tau$ , the gravitational forces  $g$  was set equal to  $0.038u_\tau^2/\delta$ .

While moving towards the wall, particles go through regions in which  $\tau_k$  decreases by a factor of three and  $v_k$  increases by approximately the same percentage. In homogeneous isotropic turbulence an appreciable increase (greater than 10%) of the settling velocity is expected for  $0.2 < \tau_p/\tau_k < 3$  when  $V_p/v_k = 1$ , and, conversely, for  $0.5 < V_p/v_k < 3$  in the case  $\tau_p/\tau_k = 1$  (Wang and Maxey 1993). The particles that move towards the wall are likely to be, at some point in their trajectories, within these ranges; however, not all the particle trajectory might fall within these critical regimes. Thus, we could expect significant differences with the results obtained in homogeneous isotropic turbulence.

To quantify the particle deposition, the following statistics were calculated: the percentage of particles that reach the wall; the relative increase of the settling velocity,  $\delta W = (w_p - W)/W$  (where  $w_p$  is the vertical component of the particle velocity); the probability-density function (*pdf*) of the streamwise distribution of the particles that have settled.  $\delta W$  is calculated considering active particles only, *i.e.*, those that have reached the walls are removed from the computation.

First, we show the time variation of  $\delta W$  (Fig. 2a), the average vertical position of the particles,  $Z$ , (Fig. 2b), and the percentage of particles that have settled (Fig. 2c) obtained from the DNS. After an initial transient ( $0 < tu_\tau/\delta < 0.1$ ) in which the particles adjust to reach the terminal velocity, a rapid increase of the settling velocity ( $0 < \delta W < 0.2$ ) is observed in a relatively short time, between  $tu_\tau/\delta = 0.1$  and  $0.5$ . At this time, no particles have reached the wall yet; their average distance from the wall is between  $0.93$  and  $0.64$ . The rapid increase of the settling velocity is due to the fact that, on average, the particles are experiencing the values of the time- and velocity-microscales responsible for the inertial bias. The  $\tau_k/\tau_p$  ratio drops from  $3.12$  at  $Z = 0.93$ , to  $1.91$  at  $Z = 0.64$ , whereas  $v_k/W$  increases from  $0.57$  to  $0.74$ . A third regime is then observed, for  $0.5 < tu_\tau/\delta < 1.2$ , characterized by a *plateau* with a maximum  $\delta W = 0.3$ . In this period some particles settle (the deposition rate is about 34% at  $tu_\tau/\delta = 1.2$ ) and their average position moves from  $Z = 0.64$  to  $0.27$ . This zone is characterized by  $1.91 > \tau_k/\tau_p > 0.92$  and  $0.74 < v_k/W < 1.05$ , and does not correspond exactly to that for which the particles experience the maximum increase of the settling velocity in homogeneous isotropic turbulence. Moreover, just as the optimum condition for the increase of the settling velocity,  $1.2 < tu_\tau/\delta < 1.55$  is about to be reached,  $\delta W$  decreases and oscillates around  $0.17$ . This fourth zone is characterized by a percentage of settled particles ranging between 34 and 55%; their average vertical position ranges between  $0.27$  to  $0.17$ . The ratio  $\tau_k/\tau_p$  continues to decrease to  $0.76$  for  $tu_\tau/\delta = 1.55$  whereas  $v_k/W$  increases up to

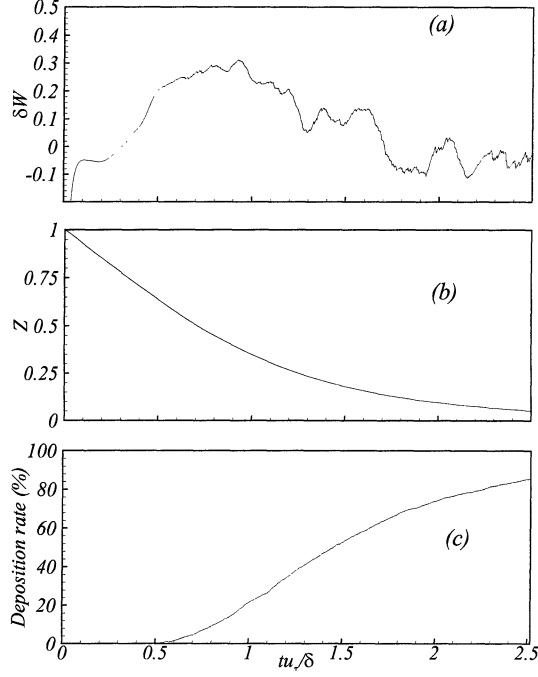


Figure 2. Particle deposition statistics calculated from the DNS. (a) Relative increase of the settling velocity; (b) average vertical position of the particles; (c) particles deposition rate.

1.15. Afterwards, the settling velocity continues to decrease and  $\delta W$  finally oscillates around the zero value.

In wall-bounded flows, more complex phenomena are occurring that overwhelm the inertial bias observed in homogeneous isotropic turbulence. For  $tu_\tau/\delta > 1.2$ , the particles are approaching the buffer layer, their average location ranging between  $Z = 0.27$  and  $Z = 0.10$  (in wall units,  $48 > Z^+ > 18$ ), and interact with the near-wall structures. While some particles are pushed towards the wall by the turbulent sweeps and settle, most are captured by turbulent bursts, and are prone to be re-ejected and re-suspended in the core of the fluid. This phenomenon, which was first observed by Pedinotti *et al.* (1990) tends to reduce the average settling velocity and also explains local negative values of  $\delta W$ .

To establish the ability of the LES to simulate particle deposition with sufficient accuracy, results of *a priori* tests will now be shown. First we have considered the particles driven by a filtered DNS field obtained by applying the filter function defined in (4) to the DNS velocity field. Two filter widths were considered,  $\Delta_i/\Delta x_i = 2$  and 3 respectively. With these meshes, the SGS contain respectively 2.2% and 8.1% of the total energy, whereas the contribution of the unresolved scales to the total dis-

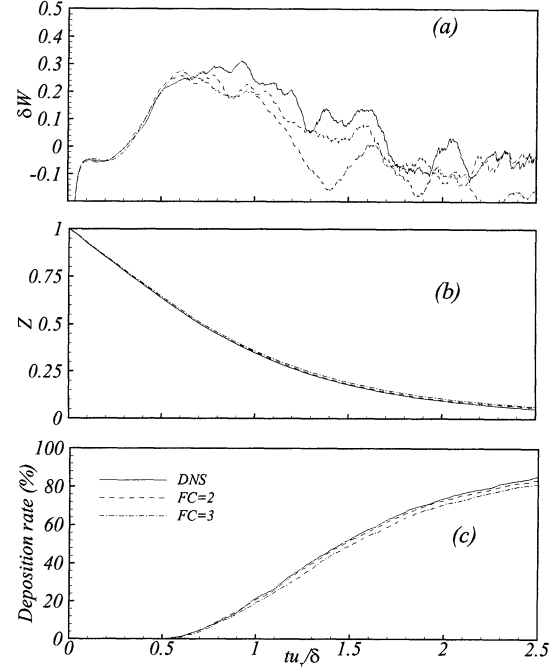


Figure 3. Comparison between DNS and filtered DNS data. (a) Relative increase of the settling velocity; (b) average vertical position of the particles; (c) particles deposition rates.

sipation ranges between the 8% and the 16%. Hereafter, the ratio  $\Delta_i/\Delta x_i = 2$  will be denoted as  $FC=2$ , the other as  $FC=3$ .

Figures 3a-c compare the time variations of  $\delta W$ ,  $Z$  and the deposition rates obtained from the DNS with those calculated moving the particles in the filtered velocity fields. Filtering always produces a reduction of  $\delta W$  (Fig. 3a). Up to  $tu_\tau/\delta \approx 0.8$  filtering does not affect the statistics significantly; the results obtained using the total or the resolved velocities agree, within the error due to the statistical sample. For  $tu_\tau/\delta > 0.8$ , however, a reduction of  $\delta W$  when the filtered field with  $FC=3$  is used can be observed. The reason for this discrepancy is unclear. It is probably not due to neglecting the effect of the small scales, since at this time the particles are still in the core of the channel, where the unresolved vorticity is not very significant; furthermore, as will be shown later, actual LES calculations that use the filter-width corresponding to  $FC=3$  do not show the dip in  $\delta W$  observed in Fig. 3. Lack of statistical convergence of the data can, however, play a role; by  $tu_\tau/\delta = 1.2$  approximately 40% of the particles have reached the wall, and have been removed from the flow, thus significantly reducing the statistical sample size.

Figures 3b,c show that the deposition phenomenon is less sensitive to filtering than the particle-settling velocity. The aver-

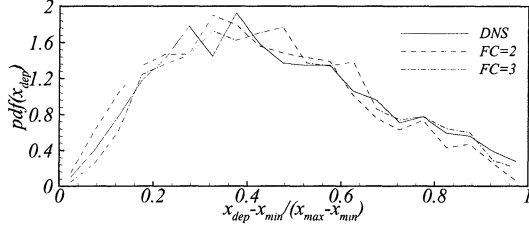


Figure 4. Probability-density function of the distribution of the settled particles along the wall evaluated using DNS and filtered DNS data.

age vertical position of the particles is not very much influenced by the filtering operation, and the maximum reduction of the deposition rate is 1.8% for the  $FC=2$  case, 4.3% for the  $FC=3$  case at  $tu_\tau/\delta = 2.5$ . The effect of filtering on the final spatial distribution of the particles can be observed from the *pdf* shown in Fig. 4. It appears that the effect of filtering on the streamwise distribution of the particles on the walls is very small.

If we compare the previous data with that obtained from two actual LES calculations (Fig. 5a), which used a fine ( $64 \times 64 \times 97$ ) and a coarse ( $48 \times 48 \times 97$ ) grid, we observe a further reduction of the settling velocity: the maximum value of  $\delta W$  for the fine-grid simulation is 0.21. LES fails to predict correctly the inertial bias, resulting in a general under-prediction of the settling velocity. The results compare better in the wall-layer, where the inertial bias is overwhelmed by the re-suspension phenomena. The results obtained with the coarse grid simulation are slightly worse than that of the finer one.

The other statistics are in better agreement with the DNS. The average vertical position of the particles and their deposition rate (Figs. 5b and c) are rather insensitive to filtering and modeling errors. Since the main effect of filtering is the reduction of the predicted settling velocity, their average vertical position is slightly reduced. At  $tu_\tau/\delta = 1.7$  the relative difference between fine LES and DNS is 8.6%, and rises to 17% for the coarse LES.

The *pdf* of the normalized distribution of settled particles in the streamwise direction is shown in Fig. 6. The distribution predicted by the LES calculations compares very well with that obtained with DNS. It has to be remarked that, although some statistics (the deposition rate, for instance), may be more sensitive to the terminal velocity than to the particle interaction with the turbulent field, the *pdf* of the particle distribution is strongly affected by the turbulent fields, and its accurate prediction is a significant achievement for engineering calculations.

#### 4 Conclusions

In the present paper an investigation of the influence of filtering and SGS modeling on the particle settling velocity has been carried out. The study has been performed using a DNS velocity

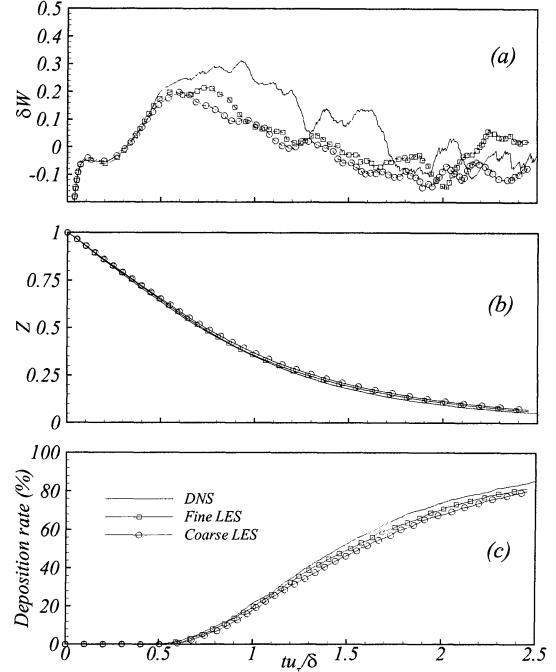


Figure 5. Comparison between DNS and LES data. (a) Relative increase of the settling velocity; (b) average vertical position of the particles; (c) particles deposition rates.

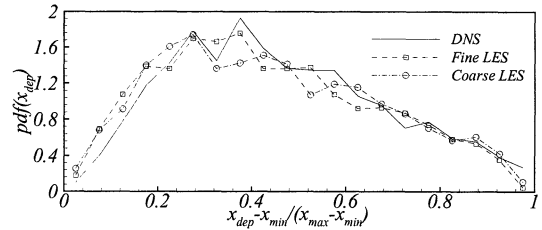


Figure 6. Probability-density function of particle along the streamwise direction evaluated with DNS and LES velocity fields.

field, two velocity fields filtered with increasing filter-width, and two LES calculations. The deposition rate, the settling velocity and the particle distribution over the wall after deposition have been evaluated and compared.

This study showed that filtering produces a reduction of the increase of settling velocity due to the inertial bias,  $\delta W$ . This reduction was observed both in the *a priori* tests and also *a posteriori*.

Other statistics are predicted more accurately: in particular,

the average position of the particles, and their distribution after deposition, were in good agreement with the DNS data. The distribution of the particles is of particular importance in many engineering applications (those that involve sediment transport, for instance), and the ability of LES to predict it accurately indicates that it may be a valuable tool for these studies.

## ACKNOWLEDGMENTS

The computations reported in the present paper were performed on the CRAY J916/8-1024 of the Computer Center of the Università di Trieste. The work was partly supported by the Ministero dell'Università e della Ricerca Scientifica e Tecnologica under the contract "Processi vorticosi, turbolenti, caotici—Applicazioni impiantistiche ed ambientali", and by the Università di Trieste under special contribution to the international research.

## REFERENCES

- Armenio, V., Piomelli, U. and Fiorotto V. Submitted to *Phys. Fluids* (1999).
- Elghobashi S., and Truesdell, G. C. *J. Fluid Mech.*, **242**, 655 (1992).
- Germano, M., Piomelli, U., Moin, P., and Cabot, W. H. *Phys. Fluids A* **3**, 1760 (1991).
- Ghosal, S., and Moin, P. *J. Comput. Phys.* **118**, 24 (1995).
- Kim, J., Moin, P., and Moser, R. D. *J. Fluid Mech.* **177**, 133 (1987).
- Lilly, D. K. *Phys. Fluids A* **4**, 633 (1992).
- Maxey, M. R. *J. Fluid Mech.*, **174**, 441 (1987).
- McLaughlin, J. B. *Phys. Fluids A* **1**, 1211 (1989).
- Murray, J. A., Piomelli, U. and Wallace, J. M. *Phys. Fluids* **8**, 1978 (1996).
- Pedinotti, S., Mariotti, G., and Banerjee, S. *Int. J. Multiphase Flow* **18**, 927 (1990).
- Reeks, M. W. *J. Fluid Mech.*, **97**, 569 (1977).
- Squires, K. D. and Eaton, J. K. *Phys. Fluids A* **3**, 1169 (1991).
- Wang, L-P. and Maxey M. R. *J. Fluid Mech.*, **256**, 27 (1993).
- Wang, Q., and Squires, K. D. *Int. J. Multiphase flow* **22**, 667 (1996).
- Wang, Q., and Squires, K. D. *Phys. Fluids* **8**, 215 (1996).
- Yang, C. Y. and Lei U. *J. Fluid Mech.*, **371**, 179 (1998).
- Yeh, F., and Lei, U. *Phys. Fluids A* **3**, 2571 (1991).
- Zang, T. A., and Hussaini, M. J. *Appl. Math. Comp.* **19**, 359 (1986).